ChemPubSoc Europe

DOI: 10.1002/open.201700132

Open Access ChemistryOPEN Full Papers

Shaping Polyyne Rods by Using an Electric Field

Esther Rozental,[a] Eli Altus,[b] Dan Thomas Major,[a] and Shmaryahu Hoz*[a]

When a homogenous electric field is applied to polyynes (C10 and C20) perpendicular to their long axis, they bend to form an arch. The height of the arch is proportional to the intensity of the electric field. The direction of the bend and its magnitude depend on the electronic nature (donor/acceptor) of the substituents at the termini of the polyyne. The driving force for the formation of the arch is the dipole moment produced in the system parallel to the electric field. This dipole moment stems from the substituents and from additional polarization by the field. The bend of the linear polyyne fits a parabolic distortion. According to mechanical engineering analysis, this results from a moment that operates at the two end zones of the polyynes, in accordance with the natural bond order (NBO) charge distribution. It is shown that solutions relevant to beam deflection due to a central load or a uniformly distributed load are not satisfactory. Various parameters, such as the dipole moment and the height of the arch, are better correlated with σ than with σ^+ or σ^-. Application of the electric field to more complex systems enables the sculpting of interesting nanoshapes.

1. Introduction

Polyynes or long carbynes can be found outside the chemical laboratory in a variety of places, from interstellar clouds[1] all the way to terrestrial plants.[2] In the laboratory, efforts have been focused on the synthesis of long polyynes. To the best of our knowledge, the longest polyyne (C44) was recently synthesized by Tykwinski et al.[3] and a C40 polyyne was synthesized by Gladysz et al.[4] Polyynes possess two impressive opposite features. Along their long axis, as we have shown, they are extremely stiff, with a Young's modulus 45 times larger than that of diamond.[5] In contrast, perpendicular to the long axis they are very flexible and easy to bend, as shown computationally and in many X-ray crystal structures.[6] Thus, bending these molecules can turn them into molecular springs. A simple thought experiment shows that if a polyyne rod (C10) is placed vertically on a table and pressed down until it buckles, with a load of 10 kcal mol^{-1}, on release it will jump to a height of 25 km ($mgh = E$). However, because nearly half of the energy is directed towards vibrational excitation, the height is reduced accordingly.[7]

In the course of our studies on the effect of electric fields on structure and reactivity,[8] we discovered that an electric field can bend a polyyne rod that has both termini fixed to an axis. Although there are many studies on the effect of electric fields on reactivity,[9] on the locomotion of nano-objects,[10] and on the mechanical[11] and electronic[12] properties of molecules, to the best of our knowledge there are very few studies of the effect of an external electric field on the shape of a molecule. Herein, we describe the formation of arches by using an electric field, and their dependence on the strength of the field and the terminal substituents.

2. Results and Discussion

2.1. Methods

The computations were performed by using the B3LYP density functional[13] 6-311++G** basis set[14] as implemented in the Gaussian 09 suit of programs.[15] The electric field intensities used were 0, 0.0025, 0.0050, 0.0075, and 0.0100 a.u., in which 1 a.u. = 5.14×10^{11} V m^{-1}. (A proton generates an electric field with a similar strength at a distance of 5 Å.) To avoid cluttering the figures too much, we retained in the legend and the axis the corresponding "Gaussian numbers" as they appeared in the command line for these fields. Namely, the corresponding value for a field strength of 0.0025 a.u. is 25 and that of 0.01 is 100.

Chains of 10 and 20 carbon atoms were examined with the following terminal substituents: NH_2, OH, Me, H, F, Cl, CF_3, CN, and NO_2. The simulations were performed in the following way: Geometry optimization was first carried out in the absence of an electric field. In the next step, the linear structure was aligned along the x axis with the first and last carbon atoms restrained to this axis ($y = z = 0$) but allowed to move free along the x axis. The electric field was applied in the posi-

[a] E. Rozental, Prof. D. T. Major, Prof. S. Hoz
Department of Chemistry and
the Institute for Nanotechnology and Advanced Materials
Bar Ilan University, Ramat Gan, 5290002 (Israel)
E-mail: shoz@biu.ac.il

[b] Prof. E. Altus
Department of Mechanical Engineering
Technion Israel Institute of Technology
Haifa, 5290002 (Israel)

Supporting Information and the ORCID identification number(s) for the author(s) of this article can be found under: https://doi.org/10.1002/open.201700132.

tive direction of the *y* axis. In this case, the *z* coordinates of all the carbon atoms were constrained to $z=0$. No constraints were applied to the substituent's atoms. Frequency calculations were performed in each case. In general, the following line of commands was used: B3LYP/6-311+G**OPT=(Z-MATRIX,CALCALL)SCF=(VeryTight, noincfock) Integral=(Grid=Ultrafine) nosymm.

2.2. Phenomenology

The bending effect of the electric field on a C10 rod is demonstrated in Figure 1 for the NH_2 substituent.

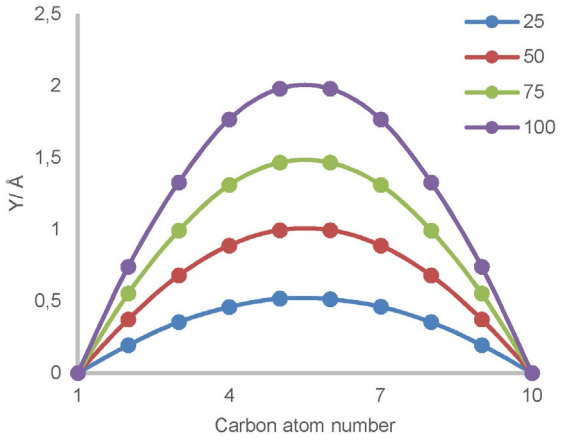

Figure 1. The *y* coordinate values of each carbon atom in a C10 rod at electric fields of 0.0025, 0.0050, 0.0075, and 0.0100 a.u. for the terminal substituent NH_2.

This figure shows the height (*y* coordinate, that is, the direction of the field) of each of the carbon atoms as a function of its position in the molecule. The direction and the amplitude of the bend depend on the substituent's ability to donate or withdraw electrons (see the Supporting Information for the other substituents). The largest bend is obtained with substituents at the two ends of the Hammett σ scale,[16] NH_2 and NO_2. Substituents F and Cl are exceptions to this general bend-direction trend. Although these are both electron-withdrawing atoms, the rods bend in the direction typical of the electron-donating substituents (Table 1).

It is conceivable that the lone-pair-donation ability of the F and the Cl substituents dictates the bend direction, however, the various system parameters correlate better with Hammett σ (mainly inductive effect) than with σ^+ or σ^-, which reflect the mesomeric effects. The reason for this deviation will be explained below. Table 1 and Figure 2 show that the height of the arch correlates with the intensity of the electric field, that is, the higher the intensity, the higher the arch.

The bend direction for the C20 rods is dictated by the substituents in the same manner as for the C10 rods, and its intensity also increases with the intensity of the electric field. However, the major difference between the two polyyne series is that, whereas the heights of the arches of the individual substituents converge for the C20 series to a value of approximately 8.5 Å (Table 1), those of the C10 series diverge according to the σ values (Figure 2).

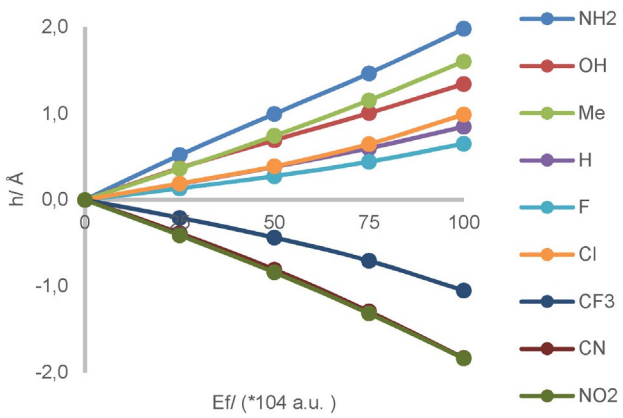

Figure 2. The height of the arch for the C10 series as a function of the electric field (Ef) strength.

It is important to note that for both the C10 and C20 series, the dipole moment is σ-dependent.

2.3. Mechanism of Bending

When a polarizable object is placed in an electric field, it undergoes polarization to minimize the energy of the system. In our case, the electric field is perpendicular to the long axis of the polyynes and, therefore, the ability of the electric field to polarize the polyyne in this arrangement is miniscule (exceptions to this are substituents NH_2 and OH, the local dipole moments of which may have a component in the direction of the field). However, because the bending of a polyyne rod is not very energetically costly,[6] bending provides an opportunity for polarization in the appropriate direction. The formation of an arch gives rise to the creation of a permanent dipole moment due to the terminal substituents. In this respect, there is a very pronounced difference between the short and long rods. Figure 3 shows, as an example, the Me-substituted C10 and the C20 rods superimposed on each other at the distortion induced by a field of 0.0075 a.u. Two important features can be

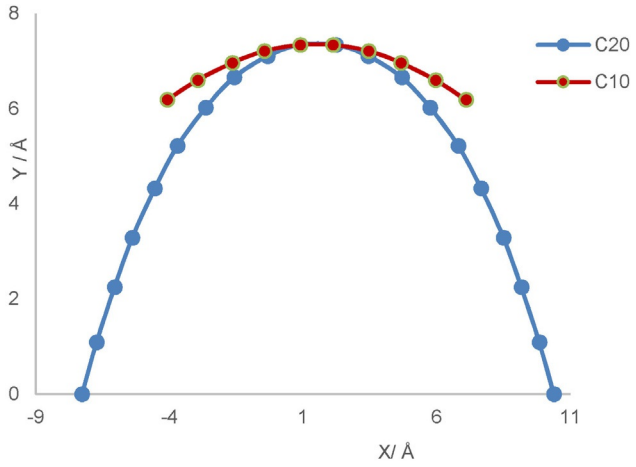

Figure 3. Superposition of the (*x*,*y*) coordinates of the Me-substituted C10 and C20 systems at a field of 0.0075 a.u.

Table 1. Substituent and electric field effects on the C10 and C20 rods.

	Field [$\times 10^4$ a.u.]	Height [Å]	Distortion energy [kcal mol^{-1}]	Dipole moment [Debye]	Dipole moment at no field [Debye]	Height [Å]	Distortion energy [kcal mol^{-1}]	Dipole moment [Debye]	Dipole moment at no field [Debye]
		C10				**C20**			
NH_2	0			1.0				0.9	
	25	0.52	0.49	3.0	2.6	3.35	1.81	8.2	6.9
	50	1.00	1.78	4.9	4.0	6.11	6.40	16.4	10.8
	75	1.47	3.84	6.8	5.2	7.84	12.23	25.5	13.1
	100	1.98	6.60	9.1	6.3	8.76	17.63	34.2	14.2
OH	0			2.3				2.3	
	25	0.37	0.34	4.2	3.8	2.16	0.77	5.8	5.8
	50	0.69	0.81	5.1	4.3	4.46	3.31	11.2	7.9
	75	1.01	1.59	6.0	4.8	6.81	7.94	18.1	9.5
	100	1.34	2.76	7.1	5.2	8.21	13.62	25.9	10.4
Me	0			0.0				0.0	
	25	0.36	0.21	1.1	0.7	2.47	0.92	3.8	2.8
	50	0.74	0.89	2.3	1.4	5.25	4.41	10.0	5.7
	75	1.15	2.11	3.7	2.1	7.34	9.76	18.1	7.5
	100	1.60	4.10	5.3	2.9	8.49	14.92	26.3	8.4
H	0			0.0				0.0	
	25	0.18	0.06	0.5	0.2	1.22	0.21	1.3	0.7
	50	0.38	0.26	1.0	0.4	3.19	1.49	3.7	1.7
	75	0.60	0.60	1.6	0.6	6.02	5.75	9.5	3.0
	100	0.85	1.19	2.2	0.9	7.90	11.57	17.0	3.7
F	0			0.0				0.0	
	25	0.13	0.01	0.4	0.1	1.05	0.16	1.1	0.5
	50	0.27	0.09	0.7	0.2	3.01	1.31	3.3	1.4
	75	0.44	0.26	1.2	0.3	6.06	6.03	9.4	2.9
	100	0.65	0.52	1.6	0.4	7.99	12.59	17.5	3.9
Cl	0			0.0				0.0	
	25	0.19	0.07	0.6	0.2	1.49	0.39	1.7	1.0
	50	0.39	0.29	1.2	0.5	4.03	2.48	5.7	2.5
	75	0.65	0.74	1.9	0.7	6.94	8.44	14.4	4.2
	100	0.99	1.64	2.8	1.0	8.38	14.52	23.6	5.0
CF_3	0			0.0				0.0	
	25	−0.21	0.10	0.8	0.3	−1.40	0.35	1.8	1.0
	50	−0.44	0.43	1.6	0.7	−3.95	2.57	5.8	2.8
	75	−0.71	1.13	2.6	1.1	−6.90	6.48	14.5	5.0
	100	−1.05	2.36	3.7	1.6	−8.43	14.07	24.1	6.5
CN	0			0.0				0.1	
	25	−0.39	0.27	1.2	0.9	−2.45	0.94	3.9	2.8
	50	−0.81	1.16	2.7	1.8	−5.49	4.95	11.3	5.8
	75	−1.29	2.91	4.5	2.7	−7.61	10.77	21.1	7.4
	100	−1.83	5.77	6.8	3.7	−8.68	15.92	30.6	8.1
NO_2	0			0.0				0.0	
	25	−0.41	0.29	1.5	1.0	−2.70	1.14	4.7	3.4
	50	−0.84	1.24	3.1	1.9	−5.76	5.73	12.9	7.1
	75	−1.32	3.06	5.0	3.0	−7.78	12.31	23.4	9.3
	100	−1.84	5.97	7.4	4.1	−8.78	18.55	33.7	10.6

discerned from this figure. The first is that the C10 rod is bent much less than the C20 rod. The second point is that the major contributors to the spatial *y* component come from the two side arms, whereas the approximately six central atoms at the top of the arch carry most of the distortion and contribute much less to the projection in the *y* direction.

Because C20 has longer side arms (formally, seven carbon atoms on each side as opposed to two in C10), it is clear that for the same electric field, it pays energetically to bend the C20 chain more than the C10 chain.

Thus, energy is invested by the field in geometric and electronic distortion and is gained by the interaction of the electric field with the permanent and induced dipoles. Both distortions, geometric and electronic, will come to a halt when an additional distortion does not yield incremental stabilization. It should be noted that the bending distortion is close to its limit for the C20 series because at an electric field of 100, the height of the arch reaches the value of approximately 9 Å, close to half the length of the rod (≈12 Å). This is probably the major cause for the convergence of height to a single value for the C20 series (Table 1), whereas the C10 series has not reached this limit and, therefore, the arch height diverges (Figure 2) according to the electronic properties of the substituents.

Also shown in Table 1 are the distortion energies calculated by comparing the energies of the bent rods in the absence of the electric field with the energies of the corresponding linear structures. The data clearly show that the C20 rods are much

more distorted than the C10 rods. This is because the distortion leads to a higher energy gain for the longer side arms. Also depicted in the table are the dipole moments of the rods, calculated in the presence and absence of the electric field. The difference between the two reflects the induced dipole, which echoes the electronic distortion that is much larger for C20. At an electric field of 0.01 a.u., the average induced dipole moment for the various C20 polyynes is (18.0 ± 3.5) Debye, whereas for C10 it is only (2.2 ± 0.75) Debye. Again, this is because of their different bending geometries.

2.4. Mechanical Engineering Considerations

We have previously shown that longitudinal compression of a polyyne rod causes, past a critical point, a buckling of the rod. As predicted by mechanical engineering, the bent rod takes the shape of a sine function. In the present case, in which the two termini of the rod are restricted to the *x* axis (to which the field is perpendicular), we explored three options: 1) a uniformly distributed load, 2) a central load, and 3) a moment (Mo) exerted at the two termini. These options are graphically depicted in Figure 4.

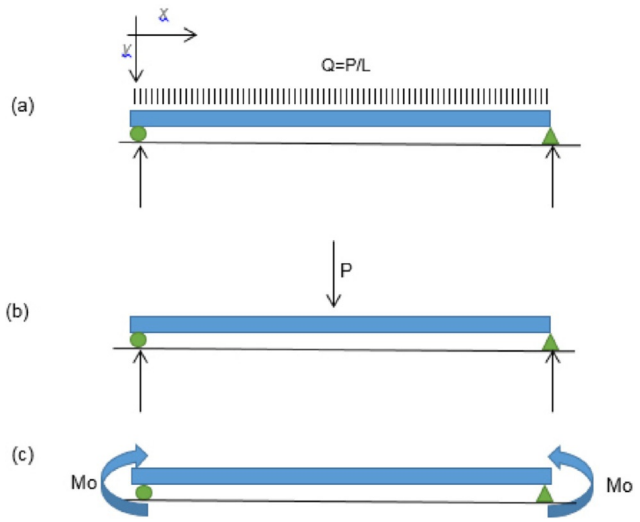

Figure 4. The three options for the forces bending the rod.

For a simply supported beam and a uniformly distributed load in the *y* direction (example 1 above), the *y* value for each nucleus is given by Equation (1):[17]

$$Y = \frac{PX}{24EI}(L^3 - 2LX^2 + X^3) \quad (1)$$

in which *P* is the external force, *L* is the length of the beam, *E* is Young's modulus, and *I* is the minimal static moment of inertia. *EI* is the bending stiffness of the beam taken from Ref. [1]. Thus, a good fitting should be obtained with a fourth-order polynomial.

The mathematical expression for the alternative case of a central load (example 2 above) is given in Equation (2):[17]

$$Y = \frac{PX}{12EI}\left(\frac{3L^2}{4} - X^2\right) \quad (2)$$

In this case, good fitting should be obtained with a third-order polynomial.

In the third case, with moments located at the ends of the rod, we have a second-order polynomial equation [Eq (3)]:[17]

$$Y = \frac{MX}{2EI}(L - X) \quad (3)$$

From our simulations, it was found that $y(x)$ fits a parabolic shape (in general r^2 values were 0.999 or higher. For a few C20 examples, r^2 values were 0.993). There was no improvement upon using a third-order polynomial and very little improvement on using a fourth-order polynomial. However, on using the normalized dimensionless variations of the equations (see the Supporting Information), it becomes evident that the system best fits a second-order polynomial. Thus, the bending of the rods seems to be due to a moment exerted at the two ends due to two pairs of forces, as shown in Figure 5.

Figure 5. Bending forces operating on the rod.

Although atomic partial charges are not physical observables, they may convey important information regarding the charge distribution in a molecule. Therefore, we performed a natural bond orbital (NBO) analysis, and inspection of the atomic charges along the chain revealed that the atomic charges are indeed concentrated mainly at the two end zones (see Figure 6 for the NH_2 substituents), which supports the notion that the major effect of the electric field stems from a bending moment at the termini of the rod.[18]

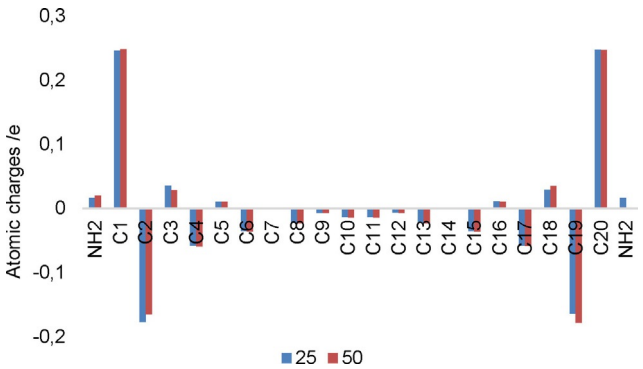

Figure 6. NBO atomic charges for C20 with NH_2 substituents at field strengths of 0.0025 and 0.0050 a.u. (H summed into N).[18]

2.5. Substituent Effect

Because of the reasons stated above, the substituent effect is mainly expressed in C10. In the C20 series, the polarization by the field is the main effect, and it largely exceeds that of substituent-induced polarization. For example, at an electric field of 0.01 a.u the dipole moment of the amino-substituted polyyne is 34.2 Debye, whereas the same bent structure outside of an electric field has a dipole moment of only 14.2 Debye. For the H-substituted system, the values were 17.0 and 3.7 Debye, respectively. Thus, the major contribution to the dipole moment comes from the electric field. In C10, conversely, in an electric field of 0.01 a.u. the amino-substituted polyyne displayed a dipole moment of 9.1 Debye, and in the absence of the field a dipole moment of 6.3 Debye was found (for the H-substituted C10 the corresponding values are 2.2 and 0.9 Debye, respectively). The difference in the expression of the substituent electronic effect (σ values, mainly inductive effect) is also nicely demonstrated in the plot of arch height versus σ for C10 and C20 at a field strength of 0.01 a.u. (Figures 7 and 8; for other fields see the Supporting Information. The Hammett equation in this and in the following cases is: Property (height, dipole moment, distortion energy) $= \sigma \times \rho + C$). The C10 series demonstrated a clear dependence on the electronic substituent effect, whereas the C20 series (apart from the direction of the bend) showed very little substituent dependence (Figure 8). Therefore, the C10 series is more suitable for the study of the substituent effect. It should also be noted that, as expected, this dependence is more pronounced at lower fields at which polarization due to the electric field contributes to a lesser degree to the dipole moment, which leads to a more pronounced substituent effect.

Interestingly, the ρ values obtained from the slopes of the plots of h versus σ correlate well with the strength of the electric field (Figure 9).

It is interesting to note that the various parameters of the system, such as height, dipole moment, and distortion energy, are, in general, better correlated with σ than with σ^+ or σ^-. This is probably due to the fact that the bonding and the antibonding orbitals are less amenable to delocalization than the benzene π orbitals, for which the various σ values were defined.

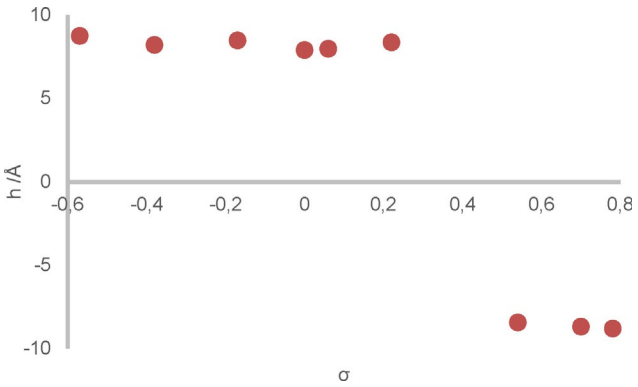

Figure 8. The arch height (h) vs. σ for C20 at 0.01 a.u. field strength.

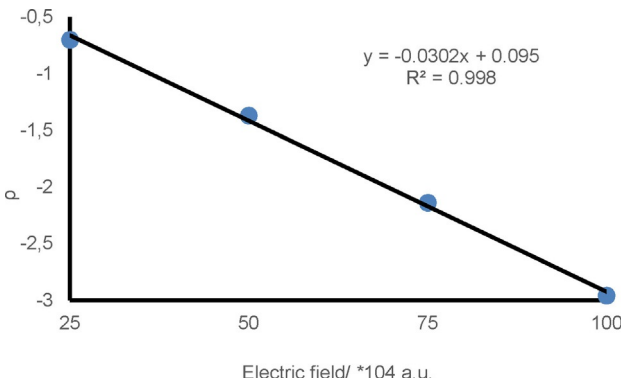

Figure 9. A plot of the dependence of the height ρ on the strength of the electric field.

A dominant feature in the Hammett-type plots for the distortion energy and the dipole moment is that the ρ values (slopes) for the electron-donating substituents are larger than those for the electron-withdrawing ones (Figures 10 and 11).

Most probably, this unusual result stems from the fact that the σ values were defined for substituents on a benzene ring, whereas in the present case the substituents reside at the ends of a set of sp carbons. Acetylenes are electron withdrawing ($\sigma = 0.2$) whereas benzenes have a σ value close to zero.[16] Thus, the chain of sp-hybridized carbons enhances the effect of the electron-donating substituents by the push-pull mecha-

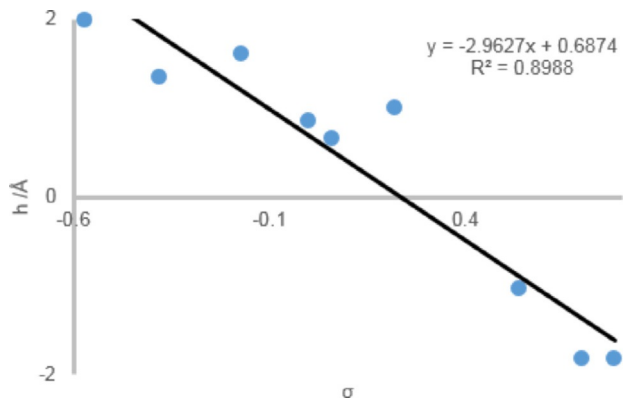

Figure 7. The arch height (h) vs. σ for C10 at 0.01 a.u. field strength.

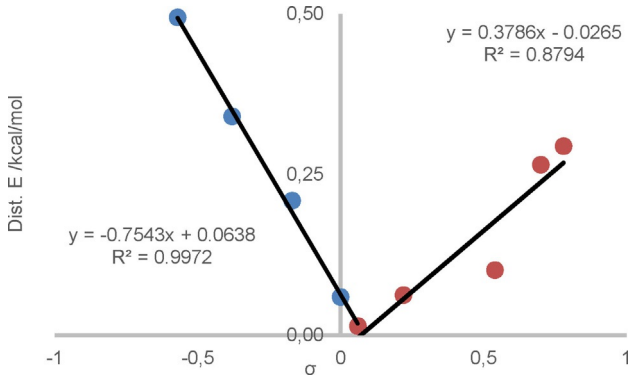

Figure 10. A Hammett-type plot for the distortion energy of C10 at an electric field strength of 0.0025 a.u.

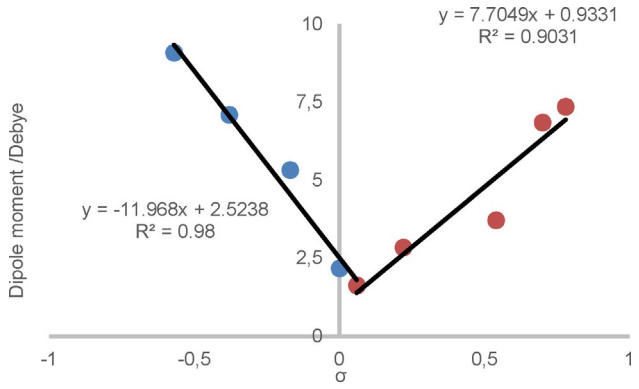

Figure 11. A Hammett-type plot for the dipole moment of C10 at an electric field strength of 0.01 a.u.

nism, whereas in the case of electron-withdrawing substituents it is more like a tug of war between the polyyne and the substituent. This pulling of electrons in opposite directions obviously reduces the dipole moment and thus also affects the distortion energy.

The above model nicely explains the fact that substituents F and Cl, although electron withdrawing in nature, cause their respective chains to bend in the same direction as the electron-donating substituents. This is because the ability to donate or withdraw electrons depends on the moiety with which the substituent interacts. In the case of a benzene ring (used for σ determination), F and Cl are indeed electron-withdrawing substituents. However, relative to an array of sp-hybridized carbons, they are electron-donating substituents and, therefore, cause the appropriate bend in the polyyne.

3. Conclusions

It should be noted that shaping by an electric field may not be limited to polyynes. Polyenes and possibly other rods made of noncarbon elements of the Periodic Table may respond to an electric field in a similar way. This may possibly be extended to WS_2 nanotubes, which are similar to carbon nanotubes and also to surfaces (graphene-like structures). In addition, electric fields may be used to generate some new and interesting architectures. An example is shown below (Figure 12, optimized at the B3LYP/6-31+G* level).

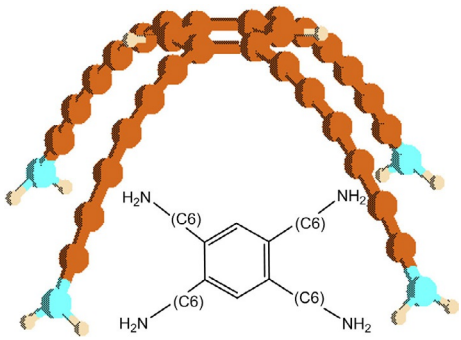

Figure 12. Electric field architecture.

Conflict of Interest

The authors declare no conflict of interest.

Keywords: ab initio calculations · electric fields · linear free-energy relationships · nanotechnology · substituent effects

[1] a) A. E. Douglas, *Nature* **1977**, *269*, 130–132; b) J. Fulara, D. Lessen, P. Freivogel, J. P. Maier, *Nature* **1993**, *366*, 439–441; c) P. Freivogel, J. Fulara, J. P. Maier, *Astrophys. J.* **1994**, *431*, L151–L154; d) J. P. Maier, *J. Phys. Chem. A* **1998**, *102*, 3462–3469; e) P. Thaddeus, M. C. McCarthy, *Spectrochim. Acta Part A* **2001**, *57*, 757–774.
[2] A. Shun, R. R. Tykwinski, *Angew. Chem. Int. Ed.* **2006**, *45*, 1034–1056; *Angew. Chem.* **2006**, *118*, 1050–1073.
[3] W. A. Chalifoux, R. R. Tykwinski, *Nat. Chem.* **2010**, *2*, 967–971.
[4] N. Weisbach, Doctoral Dissertation Universität Erlangen-Nürnberg, 2011.
[5] L. Itzhaki, E. Altus, H. Basch, S. Hoz, *Angew. Chem. Int. Ed.* **2005**, *44*, 7432–7435; *Angew. Chem.* **2005**, *117*, 7598–7601.
[6] a) A. Sakurai, M. Akita, Y. Moro-oka, *Organometallics* **1999**, *18*, 3241–3244; b) Y. H. Hu, *J. Phys. Chem. C* **2011**, *115*, 1843–1850.
[7] M. Pinchas, Y. Zeiri, S. Hoz, *Comput. Theor. Chem.* **2011**, *977*, 55–61.
[8] a) A. Yosipof, H. Basch, S. Hoz, *J. Chem. Phys. A* **2013**, *117*, 5023–5027; b) A. Yosipof, H. Basch, S. Hoz, *J. Phys. Org. Chem.* **2014**, *27*, 191–197.
[9] a) A. C. Aragonès, N. L. Haworth, N. Darwish, S. Ciampi, N. J. Bloomfield, G. G. Wallace, I. Diez-Perez, M. L. Coote, *Nature* **2016**, *531*, 88–91; b) R. Meir, H. Chen, W. Lai, S. Shaik, *ChemPhysChem* **2010**, *11*, 301–310; c) H. Hirao, H. Chen, M. A. Carvajal, Y. Wang, S. Shaik, *J. Am. Chem. Soc.* **2008**, *130*, 3319–3327; d) C. F. Gorin, E. S. Beh, Q. M. Bui, G. R. Dick, M. W. Kanan, *J. Am. Chem. Soc.* **2013**, *135*, 11257–11265.
[10] P. Calvo-Marzal, S. Sattayasamitsathit, S. Balasubramanian, J. R. Windmiller, C. Dao, J. Wang, *Chem. Commun.* **2010**, *46*, 1623–1624.
[11] M. X. Tan, W. Jo, T. Granzow, J. Frederick, E. Aulbach, J. Rödel, *Appl. Phys. Lett.* **2009**, *94*, 042909.
[12] a) H. Basch, M. A. Ratner, *J. Chem. Phys.* **2004**, *120*, 5761–5770; b) M. Wahadoszamen, T. Hamada, T. Iimori, T. Nakabayashi, N. Ohta, *J. Phys. Chem. A* **2007**, *111*, 9544–9552; c) Y. Li, J. Zhao, X. Yin, G. Yin, *J. Phys. Chem. A* **2006**, *110*, 11130–11135.
[13] a) A. D. Becke, *J. Chem. Phys.* **1993**, *98*, 5648; b) C. Lee, W. Yang, R. G. Parr, *Phys. Rev. B* **1988**, *37*, 785–789.
[14] a) K. Raghavachari, J. S. Binkley, R. Seeger, J. A. Pople, *J. Chem. Phys.* **1980**, *72*, 650–654; b) W. J. Hehre, *Acc. Chem. Res.* **1976**, *9*, 399–406.
[15] Gaussian 09, Revision A.1, M. J. Frisch, G. W. Trucks, H. B. Schlegel, G. E. Scuseria, M. A. Robb, J. R. Cheeseman, G. Scalmani, V. Barone, B. Mennucci, G. A. Petersson, H. Nakatsuji, M. Caricato, X. Li, H. P. Hratchian, A. F. Izmaylov, J. Bloino, G. Zheng, J. L. Sonnenberg, M. Hada, M. Ehara, K. Toyota, R. Fukuda, J. Hasegawa, M. Ishida, T. Nakajima, Y. Honda, O. Kitao, H. Nakai, T. Vreven, J. A. Montgomery, Jr., J. E. Peralta, F. Ogliaro, M. Bearpark, J. J. Heyd, E. Brothers, K. N. Kudin, V. N. Staroverov, R. Kobayashi, J. Normand, K. Raghavachari, A. Rendell, J. C. Burant, S. S. Iyengar, J. Tomasi, M. Cossi, N. Rega, J. M. Millam, M. Klene, J. E. Knox, J. B. Cross, V. Bakken, C. Adamo, J. Jaramillo, R. Gomperts, R. E. Stratmann, O. Yazyev, A. J. Austin, R. Cammi, C. Pomelli, J. W. Ochterski, R. L. Martin, K. Morokuma, V. G. Zakrzewski, G. A. Voth, P. Salvador, J. J. Dannenberg, S. Dapprich, A. D. Daniels, Ö. Farkas, J. B. Foresman, J. V. Ortiz, J. Cioslowski, D. J. Fox, Gaussian, Inc., Wallingford CT, **2009**.
[16] H. Maskill, *The Physical Basis of Organic Chemistry*, Oxford University Press, Oxford, **1985**.
[17] R. Parnes, *Solid Mechanics in Engineering*, Wiley, New York, **2001**.
[18] The fact that only a small amount of charge is accumulated on the NH_2 groups is in line with the observation that the system is better described by σ rather than by $\sigma+$ or σ^-.

Received: July 16, 2017
Version of record online September 12, 2017

